Imaging Studies

10

Anju Garg and M. Sarthak Swarup

Imaging plays an important role in both, the International Society of Paediatric Oncology (SIOP) as well as in the Children's Oncology Group (COG) management strategies for Wilms' tumor (WT) [1–5]. Imaging is useful for the following:

1. Detect the mass lesion and identify its organ of origin
2. Establish the initial diagnosis of WT
3. Evaluate the post-chemotherapy (preoperative) tumor response in the SIOP regimen
4. Help in staging the tumor by determining its locoregional extent and distant metastases
5. Assess the requirement of a preoperative biopsy and localization of the site for biopsy
6. Guide the biopsy wherever required
7. Postoperative follow-up for tumor recurrence
8. Surveillance of children with high risk for WT development

10.1 Imaging Modalities

The various imaging modalities available are plain radiographs of the abdomen and chest, ultrasonography (USG) with Doppler, computed tomography (CT), magnetic resonance imaging (MRI), and fluorodeoxyglucose positron emission tomography (FDG PET-CT).

10.1.1 Conventional Radiography

A plain radiograph of the abdomen is usually not included in the essential workup in the imaging protocol of WT. However, when performed, it can show evidence of a large, flank mass with the displacement of bowel loops. Calcification may be seen in less than 10% of cases [4]. Intravenous urography (IVU), which was used for many years to assess the renal mass, does not have any role in the current workup and has been replaced by ultrasound and CT/MRI as contrast-enhanced CT (CECT)/MRI provides all the information of IVU.

10.1.2 Ultrasonography

USG is often used as the first imaging modality of choice for the evaluation of children with clinical suspicion of an abdominal mass [2, 5, 6]. It can help to define the renal or extrarenal origin of the mass lesion as well as demonstrate the solid or cystic nature of the lesion. On USG, WT is visualized as a large, intrarenal, predominantly solid mass with heterogeneous and variable echotexture (Fig. 10.1) [1]. The hypoechoic and anechoic areas within the mass usually represent central necrosis or cystic degeneration, whereas

A. Garg (✉) · M. S. Swarup
Department of Radiodiagnosis, Maulana Azad Medical College and Lok Nayak Hospital, New Delhi, India

Y. K. Sarin (ed.), *Wilms' Tumor*, https://doi.org/10.1007/978-981-19-3428-5_10

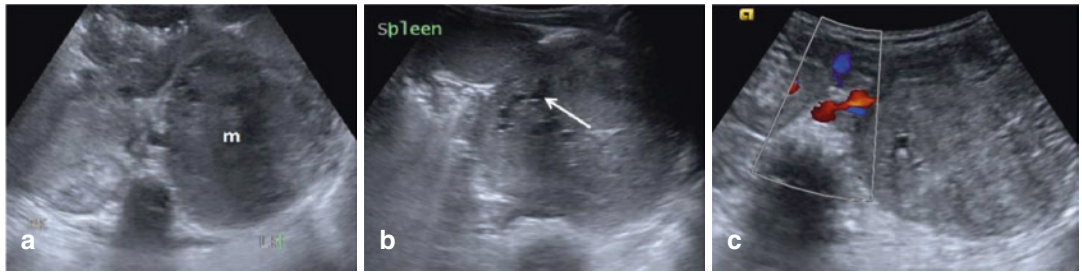

Fig. 10.1 WT in a 2-year-old girl child. Axial (**a**) and longitudinal (**b**) greyscale USG images show a large, well-defined solid heteroechoic mass lesion (m) in the left flank with small cystic areas within (arrow). Axial color Doppler USG image (**c**) shows normal color flow with patent appearing renal vein (blue)

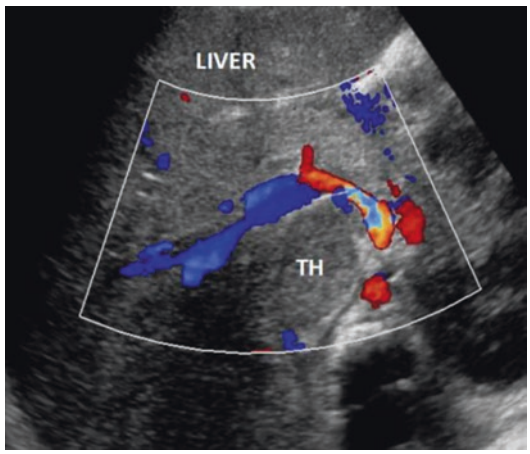

Fig. 10.2 Colour Doppler ultrasound image of a patient with WT showing intravascular extension with the thrombus (TH) in the distended IVC

echogenic areas within the mass are often due to hemorrhage and less frequently due to calcification [5, 7]. The residual renal parenchyma may be seen along the periphery of the lesion in cases presenting with large masses. A pseudocapsule can be detected on USG marginating the tumor from the rest of the renal parenchyma.

The tumor extension into the inferior vena cava (IVC) can be detected by the USG and Doppler evaluation (Fig. 10.2) [1, 5]. Intrahepatic IVC can be assessed relatively easily by Doppler; however, detection of thrombus confined only to the renal vein is relatively difficult on USG because of distortion by the tumor [7]. In cases with equivocal CT/MRI findings regarding intravascular tumor extension, Doppler sonography can act as a problem-solving tool [8]. Invasion into neighboring organs such as the liver can be evaluated by the real-time US. If the mass is seen to move freely from the organ, then invasion or adherence to the organ can be ruled out [9]. Metastases to the liver are well seen on USG. The presence, nature, and amount of fluid in the peritoneal cavity can be noted on ultrasound.

USG is good in detecting the tumor as well as the vascular extension of the lesion; however, it has a limited role in defining extra-capsular tumor spread and detecting nodal involvement and small tumors in contralateral kidneys [10]. Hence other cross-sectional imaging modalities are usually required for further characterization and determining the local tumor extent for optimal staging and operative planning [9–11].

10.1.3 Magnetic Resonance Imaging (MRI)

As per the latest UMBRELLA protocol by the Renal Tumor Study Group of the International Society of Pediatric Oncology (SIOP–RTSG), abdominal MRI is considered the preferred complementary imaging modality owing to the lack of ionizing radiation [5]. MRI is also the imaging study of choice in pediatric patients with bilateral WT or suspected bilateral tumor predisposition [2].

On MRI, WT is seen as a relatively well-defined heterogeneous lobulated mass appear-

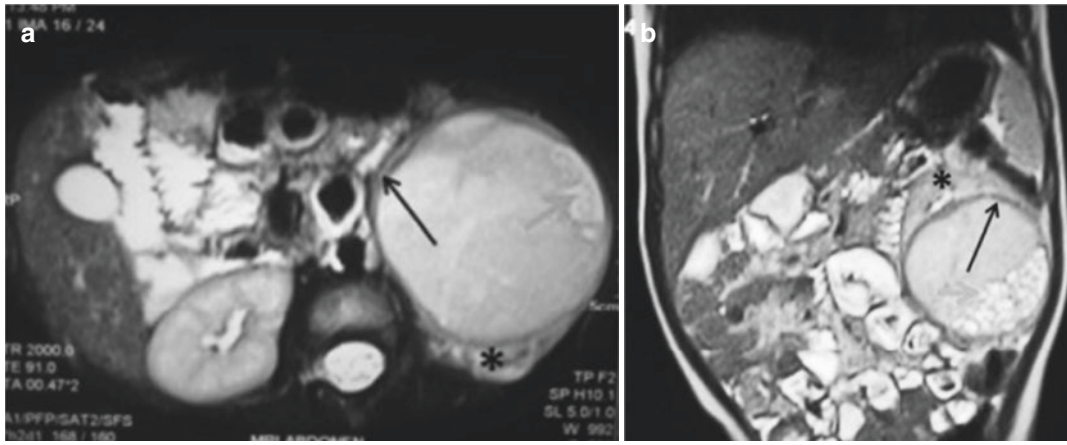

Fig. 10.3 MRI in WT in a 5-year-old male child. Axial (**a**) and coronal (**b**) T2W MR images show a well-defined hyperintense mass lesion arising from the left kidney with clawing of residual renal parenchyma (asterisk) with a hypointense pseudocapsule (black arrows). Note made of relatively more hyper-intense areas (grey arrows) within the tumor consistent with necrosis/cystic degeneration

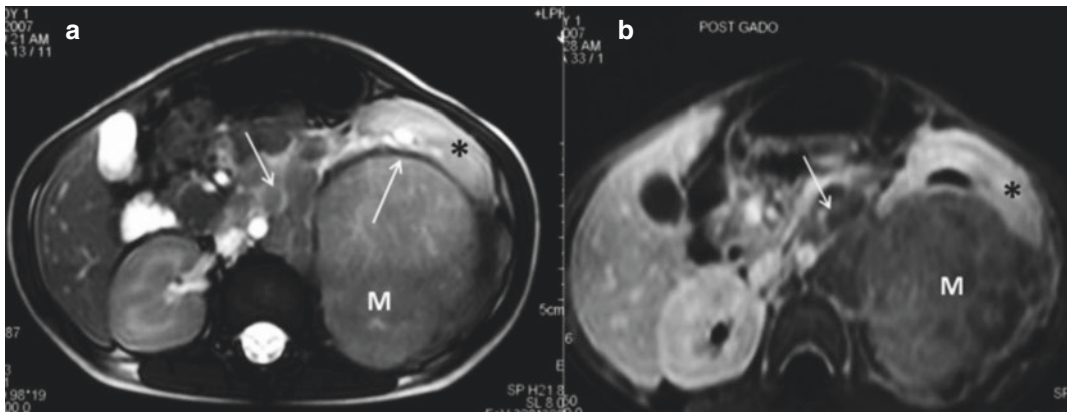

Fig. 10.4 MRI in WT in a 3-year-old girl. Axial T2W MR image (**a**) shows an iso- to hypointense mass with few focal hyperintense areas representing necrosis. The hypointense pseudocapsule (arrow in (**a**)) can be well seen separating the tumor mass (M) from the residual kidney (asterisk) which is displaced anteriorly. On the post-contrast image (**b**) the renal parenchyma (asterisk) is seen to enhance much more than the tumor mass (M). Multiple hypointense retroperitoneal lymph nodes (arrows in (**a**) and (**b**)) are seen anterior and to the left of the aorta

ing hypointense on T1W images and iso to slightly hyperintense on T2W images as compared to the normal renal cortex. Intra-tumoral necrosis and cystic changes show T2 hyperintense signal (Fig. 10.3). T1 hyperintense signal typically results from intra-tumoral hemorrhage. The pseudocapsule is seen as T1 and T2 hypointense peri-tumoral rim. The renal origin of the tumor is confirmed by the presence of a "positive beak sign" or "claw sign" which refers to the stretching and splaying of normal renal parenchyma at the periphery of the mass (Fig. 10.3). The tumors show heterogeneous postcontrast enhancement that is characteristically less as compared to normal renal parenchymal enhancement (Fig. 10.4). Gadolinium chelates in a dose of 0.1–0.2 ml/kg body weight are used as MR contrast agents.

Extension of tumor thrombus into the renal vein, IVC, and right atrium can be accurately evaluated by MRI with specific flow sequences [1, 9]. MR imaging accurately assesses the primary tumor, its size, regional extension, and relation to other organs. However, detection of subtle capsular invasion is still difficult on MRI similar to other imaging modalities. It can pick enlarged lymph nodes (LNs) (Fig. 10.4) and accurately detect focal hepatic metastatic lesions and other intra-abdominal sites of metastases [1, 9]. Small WT and nephrogenic rests (NRs) are also better detected and evaluated with gadolinium-enhanced MRI [2].

Diffusion-weighted (DW) MRI with apparent diffusion coefficient (ADC) mapping is a functional MR imaging technique that can provide additional information above conventional MRI sequences. Most malignant lesions have a high cellular density and show restricted diffusion. Hence, they show hyperintense signals on DW images. ADC is a quantitative value that decreases as the cellular density increases, and therefore, areas with diffusion restriction have low ADC values and appear hypointense on ADC maps. The DW images typically demonstrate restricted diffusion in the solid non-necrotic components of the WT [7]. DW images can differentiate viable and necrotic areas within the tumor, which is useful in selecting the optimal site for biopsy. It also helps in assessing the tumor response to neoadjuvant ChT with tumor shrinkage and increased ADC values seen in tumors responding to ChT, whereas persistently low ADC values indicate nonresponse to therapy [5]. ADC values of residual viable tumors obtained from DW images have also been found to be useful in post-ChT stratification of histological subtypes of WT (the high-risk blastemal type shows lower ADC values than various intermediate-risk subtypes) [12]. Besides this, DW imaging can be useful in detecting small synchronous tumors in the same or contralateral kidneys [2].

MR examination may sometimes become difficult to complete in children due to longer examination time with their inherent inability to lie still during the study. Sedation and in some cases general anesthesia may be necessary, which have associated risk of adverse events [5].

10.1.4 Computed Tomography

According to the SIOP-RTSG UMBRELLA protocol, CT of the abdomen for evaluation of WT should only be performed if MRI is not available [5]. However, because of its ready availability, short imaging time, and reduced need for sedation, CT is often used as the second-line imaging modality after USG.

CT examination mandates the administration of intravenous iodinated contrast for the evaluation of renal mass lesions [5]. The nonionic iodinated contrast is injected at a dose of 2 ml/kg of patient body weight. Usually, a single portal venous phase image is obtained after 65–70 s of contrast injection, which enables the opacification of venous structures including portal vein, IVC, and renal veins [13]. This single phase can provide all the information sufficient for diagnosis and staging [2, 5]. Oral contrast should be avoided as it unnecessarily prolongs the examination without providing any additional information. An extra phase—the delayed excretory phase—can be obtained in case of a small renal mass being considered for nephron-sparing surgery as this can provide information regarding the tumor's relationship with the collecting system [2].

On CT, WT appears as a large, well-defined heterogeneous mass, with a lesser degree of enhancement as compared to normal renal parenchyma. The "positive beak or claw sign" suggesting a renal origin of the mass is often well demonstrated on CECT images (Fig. 10.5). CT usually demonstrates intra-tumoral hypoattenuating areas resulting from necrosis, cystic changes, and/or fat deposition. Calcification, when present, is best seen on CT (Fig. 10.6). Exophytic growth pattern with contour irregularity may suggest capsular invasion. The renal

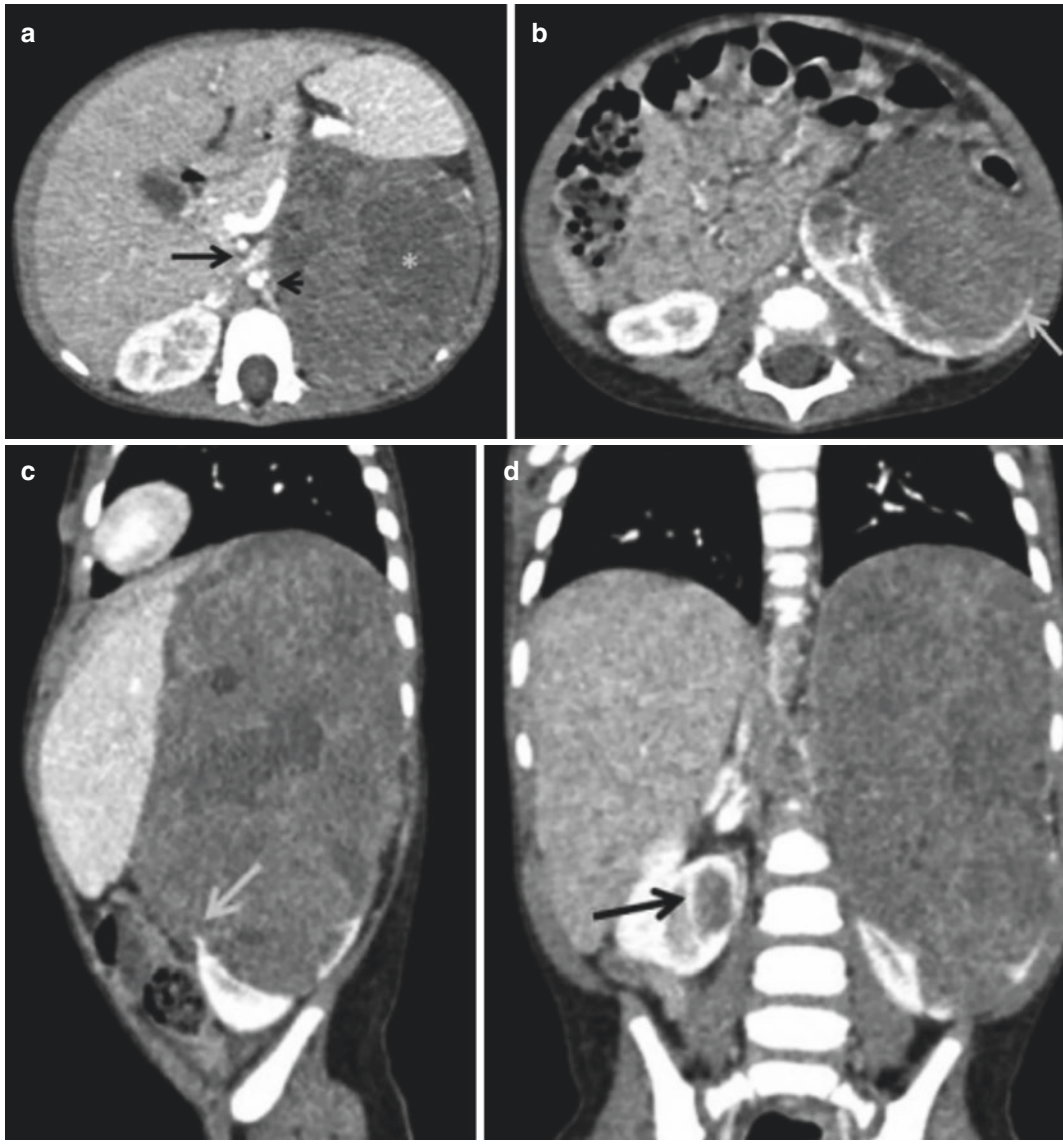

Fig. 10.5 WT of left renal origin in a 2-year-old girl. CECT axial (**a**, **b**), left parasagittal (**c**) and coronal (**d**) reformatted images show a large, well-defined, solid, hypodense, heterogeneously enhancing left flank mass with few non-enhancing areas within (asterisk in (**a**)) likely due to necrosis. The mass is causing anterior displacement of the spleen, splenic vessels, and pancreas with stretching and splaying of the residual renal parenchyma inferiorly at the lower pole showing a "positive claw sign" (grey arrow in (**b**) and (**c**)). The left renal artery (arrowhead in (**a**)) and renal vein (black arrow in (**a**)) are seen opacified in the proximal course of the lesion. A small, oval, hypodense, non-enhancing lesion seen in the lower pole of the right kidney was a nephrogenic rest (black arrow in (**d**))

veins and IVC can also be evaluated on postcontrast CT images to detect tumor thrombus extension (Fig. 10.7). CT may identify enlarged LNs; however, differentiation of neoplastic from reactive lymphadenopathy is difficult on CT. The involvement of adjacent organs, liver metastases, and the presence of intraperitoneal fluid can be well seen. CECT of the abdomen is

more sensitive than USG in defining the extent of the tumor and detecting lymph nodal, hepatic, and contralateral renal involvement. Exposure to ionizing radiation remains the main disadvantage of CT scans.

The advantages and disadvantages of USG, CT, and MRI are tabulated in Table 10.1.

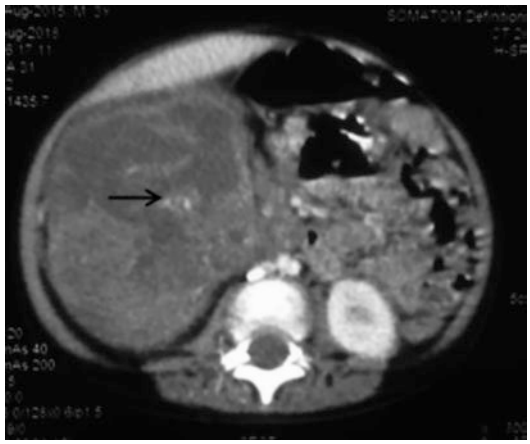

Fig. 10.6 WT in a 3-year-old boy. CECT axial image shows a large heterogeneously enhancing mass lesion arising from the right kidney with areas of necrosis. Calcific foci were seen within the tumor mass (arrow)

Table 10.1 Advantages and disadvantages of USG, CT, and MRI

Ultrasound	MRI	CT
Advantages • Noninvasive modality • Does not use ionizing radiation • Easily available • Good resolution, especially in children • Real-time evaluation • Does not require contrast or sedation	Advantages • Wide field of view • No ionizing radiation • Best soft tissue contrast resolution • Functional imaging is possible	Advantages • Wide field of view • More easily available than MRI • Short imaging time (less than 5 min) • No sedation required in older children (short sedation is required in small children)
Disadvantages • Field of view is restricted • Operator dependent	Disadvantages • May not be easily available • Long imaging time • Long sedation required • Intravenous contrast required	Disadvantages • Ionizing radiation • Intravenous contrast required

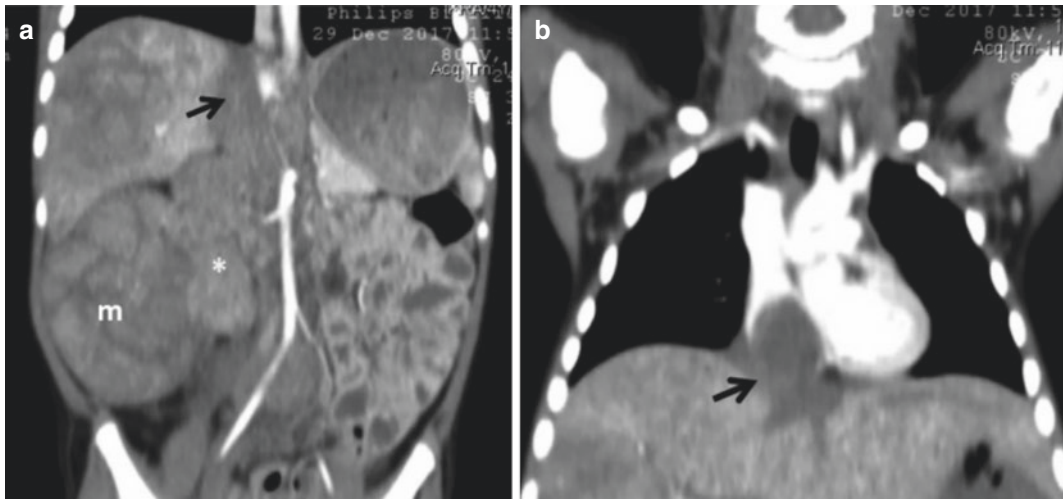

Fig. 10.7 WT in a 4-year-old girl child. Coronal CECT images of the abdomen (**a**) and Chest (**b**) show a large, heterogeneous mass of the right kidney (m) with extensive thrombosis in the right renal vein (asterisk in (**a**)) and IVC (arrow in (**a**)) extending into the right atrium (arrow in (**b**))

10.2 Tumor Staging

Staging of WT is essentially surgico-pathological. However, imaging has an important role in defining the preoperative local extent of tumor mass as this can guide surgeons while operating and assessing the distant metastases to establish the overall disease stage.

CT and MR imaging are considered to have similar accuracy in the loco-regional staging of WT [14]. Different institutions opt for either CT or MRI depending upon the availability of the imaging modality and other patient-related factors. However, MR imaging is more sensitive than CT for the evaluation of venous tumor extension and detection of contralateral synchronous lesions [5, 14, 15].

10.2.1 Local Extent

The key imaging findings that should be carefully evaluated in the abdomen include the following:

a. Infiltration of the tumor into adjacent structures.
b. Intravascular extension of tumor into the renal vein, IVC, and right atrium.
c. Detection of tumor extension into the ureter.
d. Involvement of regional lymph nodes LNs): As the size and morphology-based imaging criteria are not always accurate in differentiating benign from malignant LNs, surgical lymph nodal sampling is imperative for accurate staging [16].
e. Signs of tumor rupture (intraperitoneal and retroperitoneal): It is important to detect tumor rupture for staging and therapy planning, as it is considered an important risk factor for intra-abdominal tumor recurrence. Preoperative detection of tumor rupture on imaging may guide the surgeon in proper planning before surgery [17]. Some of the imaging findings which suggest tumor rupture include poorly defined margins of the tumor, peritumoral fat stranding, presence of fluid in retroperitoneal space, presence of significant peritoneal fluid extending beyond the cul-de-sac (irrespective of Hounsfield units), and ipsilateral pleural effusion [1, 2, 17]. Intratumoral hemorrhage, subcapsular fluid collection, or the presence of mild peritoneal fluid does not necessarily indicate tumor rupture [17]. According to the COG's current staging guidelines and SIOP-RTSG UMBRELLA protocol, imaging diagnosis of tumor rupture needs to be confirmed at the surgery and pathological examination of the nephrectomy specimen to upstage disease to stage III [2, 5].
f. Tumor spread to peritoneum: Peritoneal spread is often associated with intra-peritoneal tumor rupture. This is seen as an irregular peritoneal thickening, peritoneal nodularity, and ascites, along with mesenteric and omental solid masses on USG, CT, and MRI [4].

10.2.2 Size of the Tumor

The size of the tumor can be accurately measured on both CT and MRI. The volume of the tumor can be calculated by measuring the largest dimensions in three planes and using the formula ($A \times B \times C \times 0.523$) (Fig. 10.8). The tumor and kidney should be considered as a single unit and measured in total in a case with a large tumor, not differentiable from the kidney [5].

10.2.3 Distant Metastases

Hematogenous spread of the tumor with distant metastases is seen in approximately 20% of children with WT at the time of initial diagnosis [2]. Lungs are the most common site for distant metastases accounting for 80–85% of cases followed by the liver (Fig. 10.9) [1, 2].

10.2.3.1 Pulmonary Metastases

CT scan has largely replaced chest radiographs to assess pulmonary metastasis owing to its increased sensitivity for detecting very small lung nodules [18]. In the recent SIOP-RTSG UMBRELLA protocol recommendations, a CT chest has been made mandatory for the evaluation of pulmonary metastasis [5].

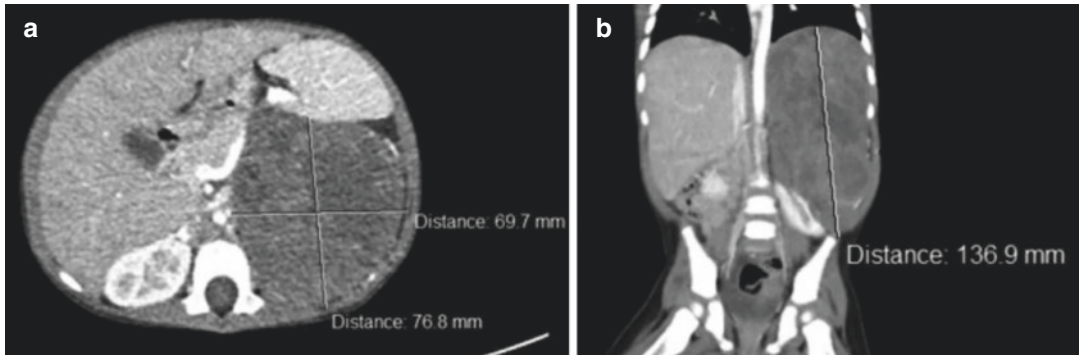

Fig. 10.8 CECT axial (**a**) and coronal (**b**) images of a child with large WT arising from the left kidney show the calculation of the volume of the lesion. The total volume of the tumor (calculated by the conventional method) was 383.2 cc

According to this guideline, intravenous contrast is not mandatory for chest CT; however, it can be used when combined with an abdominal CT scan in the same sitting [5]. It is better to perform the CT chest prior to nephrectomy as adequate evaluation of the lung parenchyma is compromised in the postoperative period by the basilar atelectasis and pleural effusions [2]. The UMBRELLA guidelines also recommend a mandatory baseline chest X-ray to be performed at initial diagnosis for comparison with follow-up chest radiographs [5].

CT-only nodules refer to small pulmonary lesions not visible on chest radiographs. There is ongoing controversy regarding staging the disease when these CT-only lesions are identified on chest CT. This is due to the fact that all CT-only nodules are not invariably metastatic deposits, and histopathological confirmation may be needed in many cases [2]. In a study under SIOP-2001 guidelines, no difference in outcome (both event-free survival and overall survival) was demonstrated between the two groups (those managed for localized disease and those managed for metastatic disease) in cases presenting with CT-only metastatic nodules [19]. On the contrary, results from the trials of Children's Oncology Group (COG), National Wilms Tumor Study Group (NWTS)-4, and NWTS-5 have demonstrated superior event-free survival (EFS) in patients with CT-only nodules and managed for metastatic disease as compared to those managed for localized disease, although the overall survival was found to be similar in both groups [5, 20, 21]. The role of chest CT in unfavorable histology or stage III disease is well established; any suspicious nodules on the CT chest should be considered significant, as accurate staging at diagnosis tends to improve overall survival in this group of patients [7, 19]. According to the latest UMBRELLA protocol, CT-only nodules larger than 3 mm in transverse diameter are managed as metastatic stage IV disease [5].

10.2.3.2 Other Metastatic Sites

About 15–20% of cases of WT can metastasize to the liver [9]. Imaging such as US, CT, and MRI can reliably detect hepatic metastases, which appear as solitary or multiple variable-sized focal lesions within the hepatic parenchyma. On USG, they are usually hyperechoic in comparison to the rest of the hepatic parenchyma (Fig. 10.9). Smaller lesions can be easily detected on CECT/MR imaging of the abdomen done for evaluation of primary tumor and typically appear as hypo-enhancing focal lesions. Metastases to the bone are very uncommon in WT and, if suspected clinically, can be detected by technetium bone scan, whole-body MRI, or FDG PET-CT.

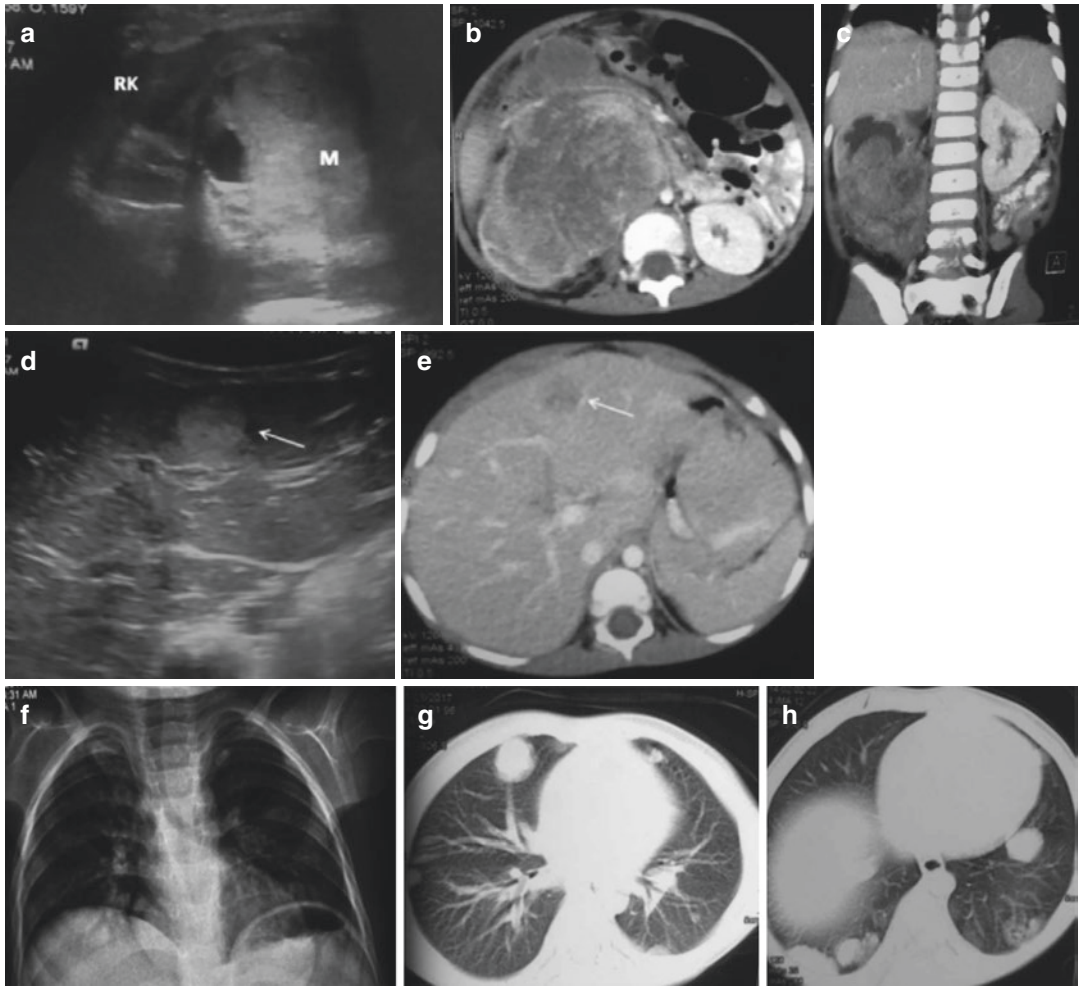

Fig. 10.9 WT in a 4-year-old boy with a history of palpable abdominal mass for 3 months with pulmonary and hepatic metastases. Greyscale USG image (**a**) shows a large, relatively well-defined, heteroechoic, solid mass lesion (M) seen arising from the mid and lower pole of the right kidney (RK). Axial (**b**) and coronal (**c**) CECT images in the same patient confirm the presence of a large, irregular, heterogeneously enhancing mass lesion arising from the mid and lower pole of the right kidney crossing midline and showing non enhancing necrotic areas within. The mass is infiltrating into the renal pelvis with resultant obstruction and dilatation of the residual upper pole calyces. Hepatic metastasis is seen as a well-defined round hyperechoic lesion (white arrow) on ultrasound (**d**) and as a round hypodense lesion (white arrow) in segment IV of the liver on CECT scan (**e**). Chest radiograph (**f**) of the same patient shows suspicious nodular opacities in the right lower zone. Axial CT sections through the chest in the lung window (**g**, **h**) reveal multiple, bilateral, rounded metastatic lesions predominantly in basal and subpleural locations

10.3 SIOP Post Chemotherapy Evaluation

SIOP protocol requires a repeat abdominal imaging preferably an MRI after completion of chemotherapy for reassessing the disease status before going to surgery. A repeat chest CT should be performed only if lung metastases were present at diagnosis [5]. Important imaging criteria to be noted are as follows:

a. *Size of the tumor*: Most of the WTs show a relative reduction in size and volume after

neoadjuvant chemotherapy. No change or increase in tumor size indicates a poor outcome. In the UMBRELLA protocol, post-ChT tumor volume has been described as a risk stratification factor for a subgroup of WTs with tumor volume >500 ml requiring aggressive treatment [5].

b. *Appearance of the tumor*: Most WTs respond by showing increased necrotic areas after ChT, appearing cystic on imaging (Fig. 10.10).

Fig. 10.10 Post-chemotherapy CECT in a case with WT of the right kidney. The tumor shows a large central necrotic component. The IVC is markedly stretched and compressed by the lesion with resultant luminal attenuation (arrow), but no evidence of intraluminal thrombus was seen

c. *Diffusion characteristics and ADC values*: There is a reduction in diffusion restriction (seen as low signal intensity on DW images) with an increase in ADC values in the responding tumor as compared to nonresponders. DWI also helps in the stratification of various histological subtypes of WT [5, 12].

10.4 Evaluation of Contralateral Kidney

It is essential to establish the status of the contralateral kidney to decide the line of management. The contralateral kidney needs to be evaluated to look for the presence of bilateral tumor (Fig. 10.11), NRs, or any co-existing renal malformations which may affect renal function. Current imaging techniques, especially MRI, are highly sensitive in detecting bilateral disease. The contralateral kidneys should be evaluated during surgery if concerning findings are evident on the preoperative imaging [2].

10.5 Nephrogenic Rests

NRs are focal, intra-renal rests, resembling the normal renal cortex on all imaging modalities. USG demonstrates large, irregularly lobulated

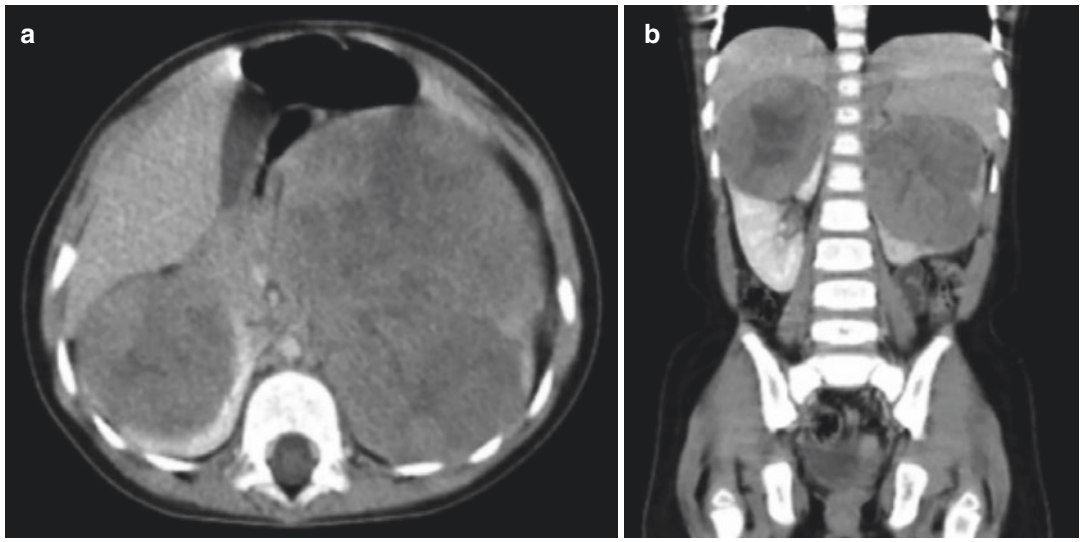

Fig. 10.11 Bilateral WT in a 2-year-old child. CECT axial (**a**) and coronal (**b**) images show two well-defined heterogeneous mass lesions involving right and left kidneys (left larger than right) with areas of necrosis within

kidneys with round or oval-shaped hypoechoic to isoechoic homogeneous renal parenchymal mass-like lesions, often with asymmetric and peripheral distribution [1]. They are better delineated on CECT and MRI as focal nonenhancing mass-like lesions (Fig. 10.5) [1]. The NRs are typically homogeneous in appearance in contrast to WTs, which tend to be heterogeneous. Diffusion-weighted imaging (DWI) can help in picking up small foci of NRs. MRI may help differentiate a sclerotic from a hyperplastic nephrogenic rest. Sclerotic rests tend to lack the potential to develop into a WT and thus considered to be in a regressive phase. CT is unable to make this distinction [22].

Multiple or diffuse nephrogenic rests are known as nephroblastomatosis (NB) [1]. The *diffuse hyperplastic perilobar nephroblastomatosis (DHPLNB)*, also known as *pan lobar NB*, is typically seen as diffuse enlargement of the kidney with a thick hypoechoic rim on USG. This abnormal tissue surrounds the renal periphery and compresses the centrally located residual parenchyma. There may be also a diffuse hyperechoic appearance of kidneys with poor corticomedullary differentiation [1]. At CT, the peripheral rim of NB is homogeneously hypodense and nonenhancing (Fig. 10.12) and causes distortion and splaying of the pelvicalyceal system and renal sinus. On MRI, it shows homogeneous hypointense signal on T1W images and variable iso- to hyperintense signal on T2W images. Contrast-enhanced images better demonstrate these lesions with sharp demarcation from the more enhancing normal renal parenchyma. Sometimes cysts may be seen along with diffuse NBL, simulating adult polycystic kidney disease. CECT and MRI are better than USG in the identification of small tumors, nephrogenic rests, and nephroblastomatosis [2, 22].

Differentiating NRs from a small WT can be difficult on imaging in some cases [2]. Increasing size on follow-up imaging, the spherical shape of the lesion, and heterogeneous enhancement are findings suspicious of neoplastic transformation [15, 23]. At present, DW imaging is unable to distinguish clearly small WT from NRs or NBL, based on mean ADC values [2, 4, 24]. However, DW images are useful in better delineation of small NR/ NB foci and detection of additional NB lesions not visible on conventional MR sequences both at the time of initial presentation and after completion of neoadjuvant ChT [4, 24].

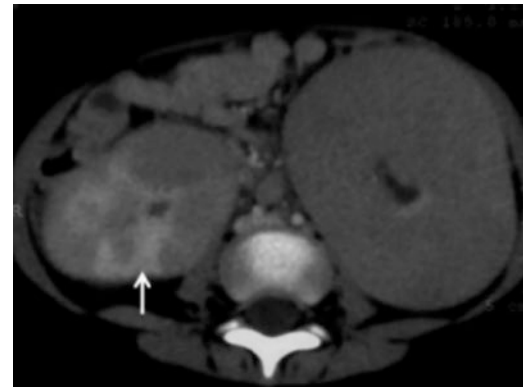

Fig. 10.12 Bilateral DHPLNB in a 1-year-old child. CECT axial image showing enlargement of bilateral kidneys (left > right) with peripheral, homogenous, nonenhancing areas almost completely replacing the normal renal parenchyma on left side. Compressed enhancing normal renal parenchyma is seen on the right side (arrow)

10.6 Role of Imaging in Nephron-Sparing Surgery

Nephron-sparing surgery (NSS) is the primary management of choice in children presenting with bilateral WT at diagnosis [1]. As already mentioned, MRI is the preferred imaging modality in these cases. In these children, DW MRI can be added to conventional MRI for improving the detection and accurately delineating the small lesions (WT, NRs, and NB). This can help the surgeons in optimizing the surgical resection to preserve the maximum possible normal renal parenchyma [4, 23, 24].

Partial nephrectomy and other forms of NSS are also considered in the management of unilateral WT in children with tumor involvement of solitary or horseshoe kidneys, in cases with contralateral genitourinary abnormalities, and in children with syndromic predisposition to develop metachronous WT in the contralateral

Table 10.2 Imaging criteria suitable for NSS [3, 5]

1	Tumor confined to single renal pole or peripheral aspect of mid-kidney
2	Unifocal tumor
3	Volume <300 ml after administration of neoadjuvant chemotherapy
4	Adequate adjacent normal renal parenchyma to achieve oncological safe margin after excision of the tumor
5	Less than 1/3 renal involvement by tumor and sparing of at least 2/3 normal renal parenchyma for function
6	No signs of preoperative rupture
7	No involvement of renal pelvis and calyces
8	Absence of obvious invasion/infiltration of surrounding organs
9	Absence of thrombus in the renal vein or IVC
10	Absence of lymph nodal involvement

kidney [1, 9]. Preoperative imaging using CT with multiplanar reconstructions or multiplanar MRI helps in identifying candidates for NSS and determining the resectability of the lesion by the accurate delineation of tumor margin and its extent [1, 5]. Features on imaging that should be assessed for the feasibility of an NSS are given in Table 10.2. Sometimes, imaging may not be able to detect normal renal parenchyma because of the volume effect of large masses, and in these cases, intraoperative US may be used to accurately delineate tumor margin during surgical excision [9].

Other imaging techniques that are useful in a patient being considered for NSS besides the usual protocol include angiography and renal functional assessment by radionuclide study. Angiographic studies may be of benefit in demonstrating vascular supply and venous drainage accurately [13]. It should ideally be performed as magnetic resonance angiography (MRA) using angiographic sequences with/without an intravascular contrast agent. Renal scintigraphy with dimercaptosuccinic acid (DMSA) is a sensitive technique for evaluating renal function and can be used for assessing the volume of functioning renal tissue. These may guide the surgeons in preserving normal functioning renal tissue while performing nephron-sparing surgery. According to the UMBRELLA protocol, isotope renography should be considered before NSS, to define the expected postoperative function, if the percentage of remnant renal parenchyma cannot be defined on conventional cross-sectional imaging [5]. Another role of imaging in NSS is the assessment of normal postoperative renal function by Doppler sonography usually performed 2 days after surgery [5].

10.7 Role of PET/PET-CT Imaging

There has been an emerging role of FDG PET-CT in the evaluation of WT. FDG avidity has been demonstrated in both primary as well as metastatic WT [3, 25]. At present, FDG PET seems to have no role in the initial diagnostic staging of WT due to the concerns of additional radiation exposure [7, 26, 27]. However, it has an important role in:

1. Evaluating the response to neoadjuvant ChT with a lower maximum standardized uptake value (SUV_{max}) demonstrated in good responders compared with poor responders to ChT [26, 27]
2. Directing biopsy from areas of active tumor activity, if it is deemed necessary [25, 28]
3. Providing additional information over and above the cross-sectional imaging studies about active residual or recurrent disease [27]
4. Accurate staging and detection of the extent of metastatic disease in children with relapse [7]

10.8 Pretreatment Biopsy

The latest SIOP-RTSG UMBRELLA protocol recommends neoadjuvant ChT to be started without biopsy confirmation, thereby increasing the importance of imaging studies in suggesting an accurate presumptive diagnosis of WT [3, 5]. However, to prevent non-WT histology from receiving an inappropriate ChT regimen, a percutaneous core needle biopsy is indicated in the presence of unusual features [5, 10, 29]. Besides unusual clinical presenta-

Table 10.3 Unusual imaging features that warrant a pretreatment biopsy [3, 5, 9, 29]

1	Presence of large lymphadenopathy
2	Presence of significant intratumoral calcifications
3	Inflammation/infiltration of psoas
4	Nonvisibility of renal parenchyma
5	Almost totally extrarenal process
6	Pulmonary metastasis in children with less than 2 years of age
7	Extrahepatic and extrapulmonary metastases

tion, that is, older than 10 years of age, urinary tract infection, septicemia, or presence of hypercalcemia, certain imaging features warrant a biopsy to confirm the histological diagnosis [3, 9, 29]. These have been tabulated in Table 10.3.

In heterogeneous tumors, imaging can help to decide the ideal site from which a biopsy should be taken [29]. The biopsy can be performed under the US or CT guidance to accurately sample from the solid and viable tumor portion, not from necrotic or cystic areas. DW MRI, as well as PET-CT, may help differentiate viable from necrotic components within tumors and therefore is useful in localizing sites for biopsy.

10.9 Differential Diagnosis

Neuroblastoma is the most important differential diagnostic consideration in children with suspected WT. WT classically demonstrates renal origin with clawing of adjacent renal parenchyma, whereas neuroblastoma is often of suprarenal origin and tends to displace the kidney. Differentiation of both these entities may be difficult at times particularly in cases with large exophytic WT and in cases with the renal invasion of neuroblastoma. Imaging morphology that favors WT is internal heterogeneity with intratumoral hemorrhage and necrosis, round to oval shape with regular margins, and lack of calcification. Abdominal neuroblastoma on the other hand usually demonstrates ill-defined margins, intratumoral calcifications, extension across the midline, displacement, and encasement of vascular structures without invasion. The presence of vascular encasement, paravertebral extension, and invasion of the spinal canal are highly suggestive of neuroblastoma, whereas demonstration of tumor invasion of renal vein and IVC strongly suggests WT [1, 7].

Other differentials of intrarenal tumors in children are renal cell carcinoma (RCC), congenital mesoblastic nephroma (CMN), clear cell sarcoma of the kidney (CCSK), and malignant rhabdoid tumor of the kidney (MRTK). These have been elaborated elsewhere in the book.

Occasionally an *infectious process* can also mimic WT—focal bacterial nephritis, xanthogranulomatous pyelonephritis (XGP) and a renal abscess may be misdiagnosed as WT. Clinical features such as fever, flank pain, urinary symptoms, and certain imaging features like the striated pattern of postcontrast enhancement or hypo-enhancing wedge-shaped areas in the adjacent renal parenchyma help distinguish infection from the tumor [1].

10.10 Posttreatment Imaging Surveillance and Screening

Approximately 15% of children treated for WT present with relapse, and most of these relapses are detected within the first 2 years after diagnosis and treatment [30]. Imaging has an important role in the posttreatment surveillance of these patients for early detection of tumor recurrence, even before the onset of symptoms, which may result in better salvage rates with the improvement of postrelapse survival [2]. The lung is the most common site of relapse for WT accounting for 50–60% of cases, followed by local or regional abdominal relapses seen in approximately 30% of cases [25, 31]. There is a higher risk of local recurrence in children with lymph nodal involvement, intraoperative tumor spillage, and unfavorable histology [28].

The duration and frequency, as well as the optimal imaging modality to be used for surveillance, are still debatable; hence, various follow-up protocols are used according to available resources and regional practices. The two most important recommendations cur-

Table 10.4 Recommendations for imaging follow-up of children with WT according to SIOP [2, 5, 8]

Patient group	Radiological investigation	Frequency after the end of therapy
Stage III and IV with high-risk histology Stage IV with Intermediate risk histology	Chest radiograph and ultrasound of the abdomen	At the end of treatment Every 2 months in 1st year Every 3 months in 2nd year Every 4 months in 3rd year Every 6 months in 4th year Annually in 5th year
All other patient groups	Chest radiograph and ultrasound of the abdomen	At the end of treatment Every 3 months in 1st and 2nd year Every 4 months in 3rd year Every 6 months in 4th year Annually in 5th year
Persistent pulmonary metastases after neoadjuvant chemotherapy	Chest CT	At the end of treatment
Bilateral tumors (stage V) and Nephrogenic rests	Chest radiograph and ultrasound of the abdomen	Every 2 months in 1st and 2nd year Every 3 months in 3rd and 4th year Annually from 5 to 10 years

rently in use for clinical and research purposes include the guidelines proposed by the COG and SIOP groups**.** The fundamental difference between SIOP and COG guidelines is that SIOP recommends chest radiographs and an abdominal USG to detect recurrence, whereas COG recommends chest CT and abdominal CT/MRI for the first 2–3 years, depending on stage of the disease and histology of the tumor, before changing to chest radiographs and abdominal USG, respectively [2]. Many recent studies have shown that imaging surveillance of treated WT cases with CT scans provides no significant advantage in terms of detection rate compared to surveillance using sonography and chest radiography while subjecting the children to a large radiation burden [32, 33]. Therefore, ultrasound and radiography-based SIOP guidelines have been preferred for clinical use in many centers. The latest SIOP-RTSG UMBRELLA protocol recommendation for imaging surveillance of WT is summarized in Table 10.4 [5, 30, 34]. Extended surveillance beyond 2 years posttreatment can be considered, but recent studies show that this approach to detect one asymptomatic relapse may not be cost-effective [30].

Children with genetic syndromes have a significantly higher risk to develop WT (>5% risk of WT) and should be screened with abdominal USG every 3–4 months. Imaging surveillance is recommended up to 5 years of age in WT1 mutant syndromes and up to at least 7 years of age in Beckwith-Wiedemann syndrome, isolated hemihypertrophy, and familial WT pedigrees [34].

10.11 Conclusion

Imaging has got an important role in the management of WT including the initial diagnosis, staging of the disease, surgical planning, posttreatment response evaluation as well as follow-up and surveillance. As the management of WT is fundamentally different in both the regimens (COG and SIOP), the imaging protocol also varies (Fig. 10.13). In both cases, a baseline imaging evaluation needs to be done at the time of initial diagnosis, which determines the renal origin of the lesion and its locoregional extent as well as detects distant metastases. As the patients in SIOP guidelines receive neoadjuvant ChT, a repeat imaging is performed after completion of ChT before proceeding to surgery. CT chest for pulmonary metastases is repeated only if pretreatment imaging showed positive findings. USG remains the initial imag-

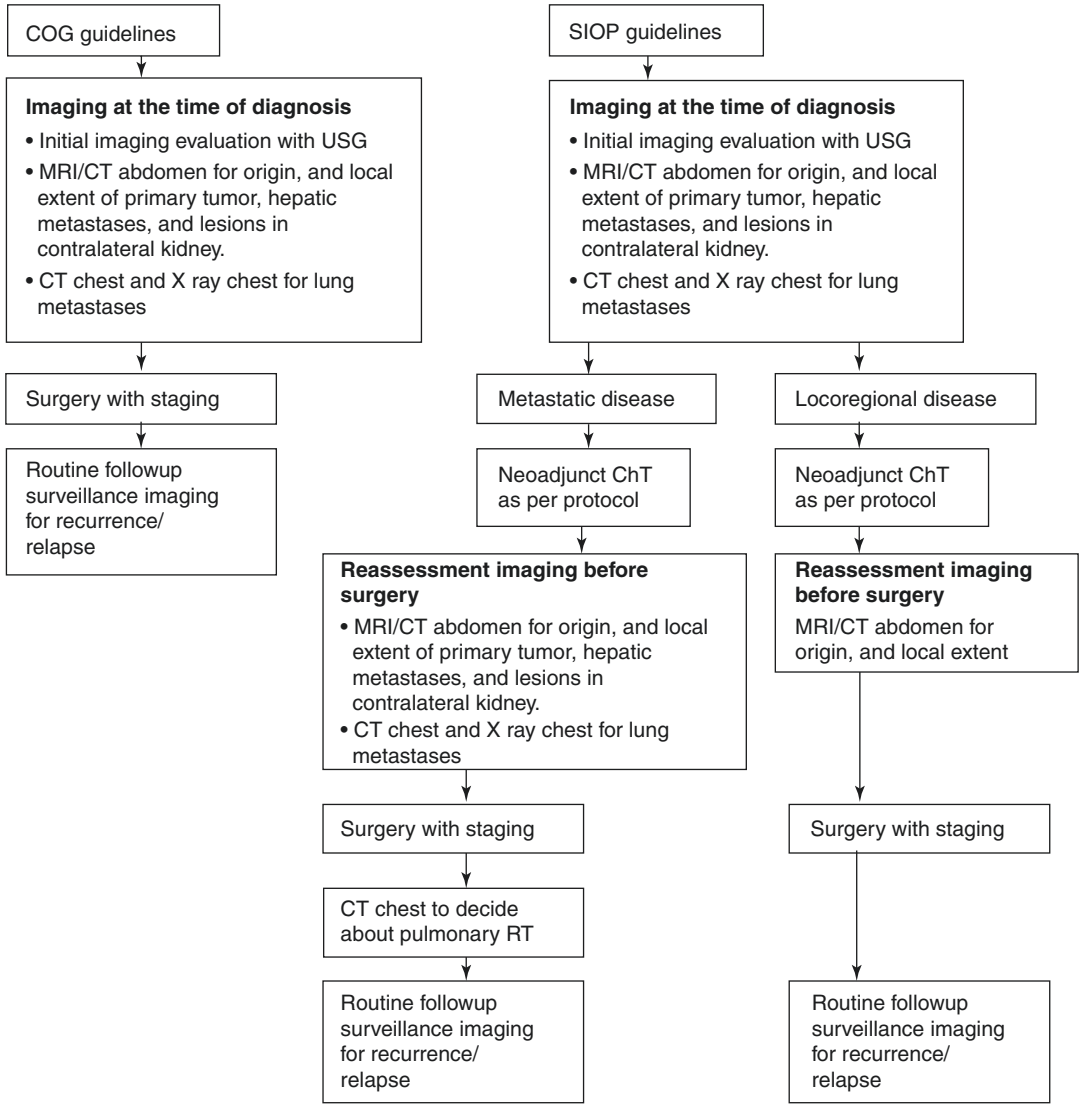

Fig. 10.13 Timing and protocol of imaging in WT according to COG and SIOP guidelines [2, 5]

ing modality of choice for the evaluation of WT. CECT and MRI are both optimal for staging and depicting the locoregional spread of the tumor, although MRI is the preferred modality due to the concerns of radiation exposure in CT. DW MRI has emerged as a promising imaging tool in recent years, as a problem-solving technique that can provide additional functional information with important management implications.

References

1. Chung EM, Graeber AR, Conran RM. Renal tumors of childhood: radiologic-pathologic correlation part 1. The 1st decade: from the radiologic pathology archives. Radiographics. 2016;36:499–522. https://doi.org/10.1148/rg.2016150230.
2. Servaes SE, Hoffer FA, Smith EA, Khanna G. Imaging of Wilms tumor: an update. Pediatr Radiol. 2019;49:1441–52. https://doi.org/10.1007/s00247-019-04423-3.

3. van den Heuvel-Eibrink MM, Hol JA, Pritchard-Jones K, van Tinteren H, Furtwängler R, Verschuur AC, et al. Position paper: rationale for the treatment of Wilms tumour in the UMBRELLA SIOP- RTSG 2016 protocol. Nat Rev Urol. 2017;14:743–52. https://doi.org/10.1038/nrurol.2017.163.
4. Brisse HJ, Smets AM, Kaste SC, Owens CM. Imaging in unilateral Wilms tumour. Pediatr Radiol. 2008;38:18–29. https://doi.org/10.1007/s00247-007-0677-9.
5. Brillantino C, Rossi E, Minelli R, Bignardi E, Coppola M, Zeccolini R, et al. Current role of imaging in the management of children with Wilms tumor according to the new UMBRELLA protocol. Transfus Med. 2019;9:206. https://doi.org/10.24105/2161-1025.9.206.
6. Davidoff AM. Wilms tumor. Adv Pediatr Infect Dis. 2012;59:247–67. https://doi.org/10.1016/j.yapd.2012.04.001.
7. Dumba M, Jawad N, McHugh K. Neuroblastoma and nephroblastoma: a radiological review. Cancer Imaging. 2015;15:5. https://doi.org/10.1186/s40644-015-0040-6.
8. Khanna G, Rosen N, Anderson JR, Ehrlich PF, Dome JS, Gow KW, et al. Evaluation of diagnostic performance of CT for detection of tumor thrombus in children with Wilms tumor: a report from the Children's Oncology Group. Pediatr Blood Cancer. 2012;58:551–5. https://doi.org/10.1002/pbc.23222.
9. Smets AM, de Kraker J. Malignant tumours of the kidney: imaging strategy. Pediatr Radiol. 2010;40:1010–8. https://doi.org/10.1007/s00247-010-1584-z.
10. McDonald K, Duffy P, Chowdhury T, McHugh K. Added value of abdominal cross-sectional imaging (CT or MRI) in staging of Wilms' tumours. Clin Radiol. 2013;68:16–20. https://doi.org/10.1016/j.crad.2012.05.006.
11. Aldrink JH, Heaton TE, Dasgupta R, Lautz TB, Malek MM, Abdessalam SF, et al. Summary article: update on Wilms tumor. J Pediatr Surg. 2019;54:390–7. https://doi.org/10.1016/j.jpedsurg.2018.09.005.
12. Littooij AS, Nikkels PG, Hulsbergen-van de Kaa CA, van de Ven CP, van den Heuvel-Eibrink MM, Olsen ØE. Apparent diffusion coefficient as it relates to histopathology findings in post-chemotherapy nephroblastoma: a feasibility study. Pediatr Radiol. 2017;47:1608–14. https://doi.org/10.1007/s00247-017-3931-9.
13. McHugh K, Fairhurst J. Paediatric neoplasms. In: Nicholson T, editor. Recommendations for cross-sectional imaging in cancer management. 2nd ed. London: The Royal College of Radiologists; 2014.
14. Servaes S, Khanna G, Naranjo A, Geller JI, Ehrlich PF, Gow KW, et al. Comparison of diagnostic performance of CT and MRI for abdominal staging of pediatric renal tumors: a report from the Children's Oncology Group. Pediatr Radiol. 2015;45:166–72. https://doi.org/10.1007/s00247-014-3138-2.
15. Lowe LH, Isuani BH, Heller RM, Stein SM, Johnson JE, Navarro OM, et al. Pediatric renal masses: Wilms tumor and beyond. Radiographics. 2000;20:1585–603. https://doi.org/10.1148/radiographics.20.6.g00nv051585.
16. Gow KW, Roberts IF, Jamieson DH, Bray H, Magee JF, Murphy JJ. Local staging of Wilms' tumor-computerized tomography correlation with histological findings. J Pediatr Surg. 2000;35:677–9. https://doi.org/10.1053/jpsu.2000.5941.
17. Khanna G, Naranjo A, Hoffer F, Mullen E, Geller J, Gratias EJ, et al. Detection of preoperative Wilms tumor rupture with CT: a report from the Children's Oncology Group. Radiology. 2013;266:610–7. https://doi.org/10.1148/radiol.12120670.
18. Irtan S, Ehrlich PF, Pritchard-Jones K. Wilms tumor: "State-of-the art" update, 2016. Semin Pediatr Surg. 2016;25:250–6. https://doi.org/10.1053/j.sempedsurg.2016.09.003.
19. Smets AM, van Tinteren H, Bergeron C, De Camargo B, Graf N, Pritchard-Jones K, et al. The contribution of chest CT-scan at diagnosis in children with unilateral Wilms' tumour: results of the SIOP 2001 study. Eur J Cancer. 2012;48(7):1060–5. https://doi.org/10.1016/j.ejca.2011.05.025.
20. Grundy PE, Green DM, Dirks AC, Berendt AE, Breslow NE, Anderson JR, et al. Clinical significance of pulmonary nodules detected by CT and Not CXR in patients treated for favorable histology Wilms tumor on national Wilms tumor studies-4 and -5: a report from the Children's Oncology Group. Pediatr Blood Cancer. 2012;59:631–5. https://doi.org/10.1002/pbc.24123.
21. Dome JS, Graf N, Geller JI, Fernandez CV, Mullen EA, Spreafico F, et al. Advances in Wilms tumor treatment and biology: progress through international collaboration. J Clin Oncol. 2015;33:2999–3007. https://doi.org/10.1200/JCO.2015.62.1888.
22. Rohrschneider WK, Weirich A, Rieden K, Darge K, Troger J, Graf N. US, CT and MR imaging characteristics of nephroblastomatosis. Pediatr Radiol. 1998;28:435–43. https://doi.org/10.1007/s002470050378.
23. Charlton J, Irtan S, Bergeron C, Pritchard-Jones K. Bilateral Wilms tumour: a review of clinical and molecular features. Expert Rev Mol Med. 2017;19:e8. https://doi.org/10.1017/erm.2017.8.
24. Platzer I, Li M, Winkler B, Schweinfurth P, Pabst T, Bley T, et al. Detection and differentiation of paediatric renal tumours using diffusion-weighted imaging: an explorative retrospective study. Cancer Res Front. 2015;1:178–90. https://doi.org/10.17980/2015.178.
25. Grundy P, Perlman E, Rosen NS, Warwick AB, Glade Bender J, Ehrlich P, et al. Current issues in Wilms tumor management. Curr Probl Cancer. 2005;29:221–60. https://doi.org/10.1016/j.currproblcancer.2005.08.002.
26. Begent J, Sebire NJ, Levitt G, Brock P, Jones KP, Ell P, et al. Pilot study of F(18)-fluo-rodeoxyglucose positron emission tomography/computerised tomography in Wilms' tumour: correlation with conventional

imaging, pathology and immunohistochemistry. Eur J Cancer. 2011;47:389–96. https://doi.org/10.1016/j.ejca.2010.09.039.
27. Qin Z, Tang Y, Wang H, Cai W, Fu H, Li J, et al. Use of 18F-FDG-PET-CT for assessment of response to neo-adjuvant chemotherapy in children with Wilms tumor. J Pediatr Hematol Oncol. 2015;37:396–401. https://doi.org/10.1097/MPH.0000000000000323.
28. Shamberger RC, Guthrie KA, Ritchey ML, Haase GM, Takashima J, Beckwith JB, et al. Surgery-related factors and local recurrence of Wilms tumor in National Wilms Tumor Study 4. Ann Surg. 1999;229(2):292–7. https://doi.org/10.1097/00000658-199902000-00019.
29. de la Monneraye Y, Michon J, Pacquement H, Aerts I, Orbach D, Doz F, et al. Indications and results of diagnostic biopsy in pediatric renal tumors: a retrospective analysis of 317 patients with critical review of SIOP guidelines. Pediatr Blood Cancer. 2019;66:e27641. https://doi.org/10.1002/pbc.27641.
30. Brok J, Lopez-Yurda M, Tinteren HV, Treger TD, Furtwängler R, Graf N, et al. Relapse of Wilms' tumour and detection methods: a retrospective analysis of the 2001 Renal Tumour Study Group–International Society of Paediatric Oncology Wilms' Tumour Protocol Database. Lancet Oncol. 2018;19:1072–81. https://doi.org/10.1016/S1470-2045(18)30293-6.
31. Malogolowkin M, Spreafico F, Dome JS, van Tinteren H, Pritchard-Jones K, van den Heuvel-Eibrink MM, et al. Incidence and outcomes of patients with late relapse of Wilms' tumour. Pediatr Blood Cancer. 2013;60:1612–5. https://doi.org/10.1002/pbc.24604.
32. Otto JH, Janse van Rensburg J, Stones DK. Post-treatment surveillance abdominopelvic computed tomography in children with Wilms tumour: is it worth the risk? S Afr J Rad. 2015;19:784. https://doi.org/10.4102/sajr.v19i1.784.
33. Mullen EA, Chi YY, Hibbitts E, Anderson JR, Steacy KJ, Geller JI, et al. Impact of surveillance imaging modality on survival after recurrence in patients with favorable-histology Wilms tumor: a report from the Children's Oncology Group. J Clin Oncol. 2018;18:1800076. https://doi.org/10.1200/JCO.18.00076.
34. Scott RH, Walker L, Olsen ØE, Levitt G, Kenney I, Maher E, et al. Surveillance for Wilms tumour in at-risk children: pragmatic recommendations for best practice. Arch Dis Child. 2006;91:995–9. https://doi.org/10.1136/adc.2006.101295.